Journal of Power Sources 260 (2014) 159–162

Contents lists available at ScienceDirect

Journal of Power Sources

journal homepage: www.elsevier.com/locate/jpowsour

Short communication

Soft chemical synthesis and the role of potassium pentahydrogen bis(phosphate) in a proton conducting composite electrolyte based on potassium dihydrogen phosphate

Chung-Yul Yoo*, Si Young Jang, Jong Hoon Joo, Ji Haeng Yu, Jong-Nam Kim*

Korea Institute of Energy Research, 152 Gajeong-ro, Yuseong-gu, Daejeon 305-343, Republic of Korea

HIGHLIGHTS

- Proton conducting phosphates have been prepared by using a wet impregnation method.
- Crystalline $KH_5(PO_4)_2$ is introduced to proton conducting electrolyte based on KH_2PO_4.
- Molten $KH_5(PO_4)_2$ plays a decisive role in increasing the proton conductivity.
- SiO_2 addition ensures long-term viability under relatively low humidification.

ARTICLE INFO

Article history:
Received 23 January 2014
Received in revised form
7 March 2014
Accepted 8 March 2014
Available online 16 March 2014

Keywords:
Proton conductor
Solid acid
Phosphate
Composite electrolyte
Fuel cell

ABSTRACT

Proton conducting composites based on potassium dihydrogen phosphate (KH_2PO_4) have been successfully prepared and characterized as a potential electrolyte for intermediate temperature fuel cells. X-ray diffraction, thermal analysis, and conductivity measurements reveal that the molten potassium pentahydrogen bis(phosphate) ($KH_5(PO_4)_2$) phase enhances the proton conductivity of KH_2PO_4–$KH_5(PO_4)_2$ composites by more than four orders of magnitude. The addition of 10 wt.% SiO_2 is sufficient to alleviate the dehydration of KH_2PO_4–$KH_5(PO_4)_2$, and long-term stable conductivity is exhibited under a relatively low humidification level (pH_2O = 0.03 atm).

1. Introduction

Solid acid phosphates, $M_aH_b(PO_4)_c$ (M = K, Rb, Cs; *a*, *b*, *c* = integer), have potential for use as electrolytes for intermediate-temperature fuel cells at 100–200 °C [1–9]. The state of the art proton conducting solid acid phosphates is caesium dihydrogen phosphate (CsH_2PO_4). The conductivity of CsH_2PO_4 above the superprotonic phase transition temperature (~230 °C) increases by more than two orders of magnitude, exhibiting conductivity of about 10^{-2} S·cm^{-1}. The implementation of CsH_2PO_4 electrolytes in fuel cells is restricted due to costly Cs and the requirement of a high humidification condition ($pH_2O \geq 0.3$ atm) to avoid dehydration. Since solid acid phosphates are highly soluble in water, the management of water vapor is required to prevent condensed water from contacting the electrolyte in case of fuel cell shut-down.

To overcome the aforementioned problems of CsH_2PO_4, a potassium dihydrogen phosphate (KH_2PO_4) base electrolyte has been studied as an alternative. However, the use of KH_2PO_4 is still limited due to its poor proton conductivity of about 10^{-4}–10^{-6} S·cm^{-1} in a temperature range of 100–200 °C even under high pressure (1 GPa) [9] and high humidity (pH_2O = 0.3 atm) [10]. Eguchi et al. attempted to enhance the proton conductivity of KH_2PO_4 [10]. They found that the proton conductivity of a KH_2PO_4/SiP_2O_7 composite can be significantly enhanced (e.g., 0.04 S·cm^{-1} at 220 °C and pH_2O = 0.3 atm) by the formation of molten potassium pentahydrogen bis(phosphate) ($KH_5(PO_4)_2$) at the interface between KH_2PO_4 and SiP_2O_7 from the chemical reaction of KH_2PO_4 and SiP_2O_7 at 220 °C. However, no direct evidence of the formation of molten $KH_5(PO_4)_2$ has been found because the molten phase cannot be detected by X-ray diffractometry. In addition, stability under low humidification (pH_2O ~ 0.03 atm) has not been reported. This

* Corresponding authors. Tel.: +82 42 860 3083; fax: +82 42 860 3133.
E-mail addresses: cyoo@kier.re.kr, chungyulyoo@gmail.com (C.-Y. Yoo), jnkim@kier.re.kr (J.-N. Kim).

http://dx.doi.org/10.1016/j.jpowsour.2014.03.019
0378-7753/

background has inspired us to explore a direct synthetic method of a $KH_5(PO_4)_2$ containing electrolyte based on KH_2PO_4 and a stabilization route under a relatively low humidification level. In this study, we successfully demonstrate that crystalline $KH_5(PO_4)_2$ is introduced to a proton conducting electrolyte based on KH_2PO_4 by using a wet impregnation method and that the addition of SiO_2 in the electrolyte ensures long-term viability for use below 200 °C under relatively low humidification ($pH_2O = 0.03$ atm). To the best of our knowledge, this is the first report on a soft chemical method for the synthesis of $KH_5(PO_4)_2$ phase in a composite electrolyte based on KH_2PO_4.

2. Experimental

KH_2PO_4–$KH_5(PO_4)_2$ powder was prepared by the dropwise addition of water-based phosphoric acid (85 wt.%, OCI) to an aqueous solution of KOH (Junsei, ultra-pure) under rigorous stirring followed by slow evaporation of water at room temperature. The molar ratio of phosphoric acid to KOH is 1:1. KH_2PO_4–$KH_5(PO_4)_2$–SiO_2 powders were prepared using a wet impregnation method. Amorphous fumed SiO_2 powder with a particle size of ~ 7 nm (Sigma–Aldrich) was suspended in an aqueous solution of KH_2PO_4–$KH_5(PO_4)_2$ under rigorous stirring, containing 5 wt.% and 10 wt.% of SiO_2. Water was removed by slow evaporation of the suspensions. The obtained powders were dried at 120 °C for 12 h, ground in agate mortar, and stored in a desiccator. The crystal phase was analyzed by step scan X-ray diffraction (Rigaku D/MAX 2200) in the range 15–50° using 5 s count time at increments of 0.02° at room temperature and processed with the JADE program. Thermal analysis of the powders was conducted from room temperature to 500 °C under flowing dry Ar with a heating rate of 5 °C·min^{-1} using a TG-DTA system (SDT 2960, TA instrument). High temperature X-ray diffraction (Rigaku D/MAX 2500) measurements were also performed by continuous scan at a scan speed of 0.02 per second under flowing dry Ar in a temperature range of 100–180 °C. Equilibration was considered completed at each temperature when no shift was found in the positions of diffraction peaks.

For conductivity measurements, about 0.9 g of powder was uniaxially pressed at 25 MPa into discs (20 mm diameter, 12 mm thickness), followed by cold isostatic pressing at 300 MPa with Ag electrodes (Elcoat). Temperature dependence of conductivity was measured by AC impedance spectroscopy (Autolab, Metrohm) during heating. The applied frequency was in a range of 1 MHz to 0.1 Hz with an excitation voltage of 50 mV. The measurements were conducted from 100 to 180 °C under a 3% H_2O/Ar atmosphere. The sample was equilibrated for 0.5 h before data acquisition to achieve equilibrium. A preliminary fuel cell test was performed using a Ag electrodes (Elcoat) and commercial Pt/C electrodes (EC1019-2, 0.5 mg·cm^{-2}, Fuel Cell Earth) to investigate the open circuit voltage. Dry air was fed to the cathode side while hydrogen was supplied to the anode side.

3. Results and discussion

Fig. 1 shows the room temperature X-ray diffraction patterns of KH_2PO_4–$KH_5(PO_4)_2$ and KH_2PO_4–$KH_5(PO_4)_2$–SiO_2 composites with 5 wt.% and 10 wt.% mass fractions of SiO_2. All patterns are assigned to orthorhombic KH_2PO_4 [11] and monoclinic $KH_5(PO_4)_2$ [12]. The calculated X-ray diffraction patterns of KH_2PO_4 and $KH_5(PO_4)_2$ are shown in the Supporting information (Fig. S1). The formation of $KH_5(PO_4)_2$ might be attributed to local rapid heating of the solution due to the acid–base reaction between KOH and H_3PO_4. The exothermic heat from the reaction could lead to inhomogeneity in the preparation solution. No evidence of the presence of other phases is found in the X-ray diffraction patterns.

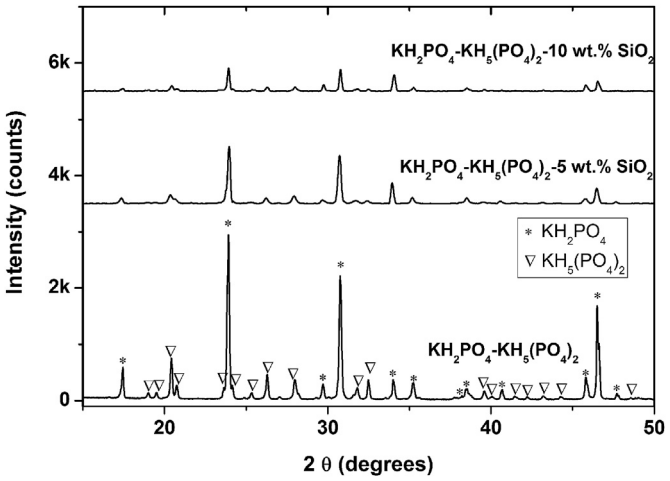

Fig. 1. Room temperature X-ray diffraction patterns of KH_2PO_4–$KH_5(PO_4)_2$–SiO_2 composites with 0 wt.%, 5 wt.%, and 10 wt.% of SiO_2.

The addition of amorphous SiO_2 (See Fig. S2 in the Supporting information) induces a loss of intensity and broadening of the diffraction peaks, which are due to the loss of crystallinity and amorphization of KH_2PO_4 and $KH_5(PO_4)_2$ phases. This might be attributable to infiltration of KH_2PO_4 and $KH_5(PO_4)_2$ in the pores of well-dispersed SiO_2 particles during the preparation, since the powder volume of commercial fumed SiO_2 (powder density ~ 0.037 g·cm^{-3}) is much larger than those of KH_2PO_4 (theoretical density = 2.35 g·cm^{-3}) and $KH_5(PO_4)_2$ (theoretical density = 2.13 g·cm^{-3}). Similar results have been found in previous studies of solid acid-SiO_2 composites [13–18].

Fig. 2 shows the results of thermogravimetry (TG) and differential thermal analyses (DTA) for KH_2PO_4–$KH_5(PO_4)_2$ and SiO_2 composites under dry Ar. The onset temperature of weight loss decreases from 150 °C to 145 °C by increasing the SiO_2 mass fraction due to partial dehydration of the powders. A possible explanation is that the presence of a SiO_2 dispersoid-solid acid interface reduces the number of hydrogen bonds in the hydrogen-bonded PO_4 accompanying a decrease of the dehydration temperature of solid acids. Consistent with the TG analysis, the first endothermic peak position in the DTA curve decreases from 130 °C to 125 °C. In contrast to all prepared powders, the as-received KH_2PO_4 (Sigma–Aldrich) does not show an endothermic peak below 200 °C. Supplementary high temperature X-ray diffraction measurements have been conducted to investigate the phase behavior of KH_2PO_4–$KH_5(PO_4)_2$ and 10 wt.% SiO_2 composite. As shown in Fig. 3, high temperature X-ray diffraction measurements confirm that the crystallinity of the $KH_5(PO_4)_2$ phase completely vanished above 130 °C for KH_2PO_4–$KH_5(PO_4)_2$ and 125 °C for 10 wt.% SiO_2 composite; hence the first endothermic peak in the DTA curve corresponds to the melting of $KH_5(PO_4)_2$. The high temperature X-ray diffraction study also reveals that *i*) the crystallinity loss is found for KH_2PO_4 without any secondary phase formation due to the dehydration and *ii*) the peak splitting of KH_2PO_4 phase is observed upon heating at temperature higher than 125 °C for KH_2PO_4–$KH_5(PO_4)_2$ and 100 °C for 10 wt.% SiO_2 composite. The observed peak splitting of KH_2PO_4 can be attributed to the formation of metastable KH_2PO_4 phase since it has been found that the metastable $P2_1/c$ phase of KH_2PO_4 can be formed upon heating and coexist with the dehydration products of KH_2PO_4 [19,20]. The endothermic weight loss above 200 °C for all measured samples is attributed to the formation of KPO_3 accompanied by multiple dehydration steps [9].

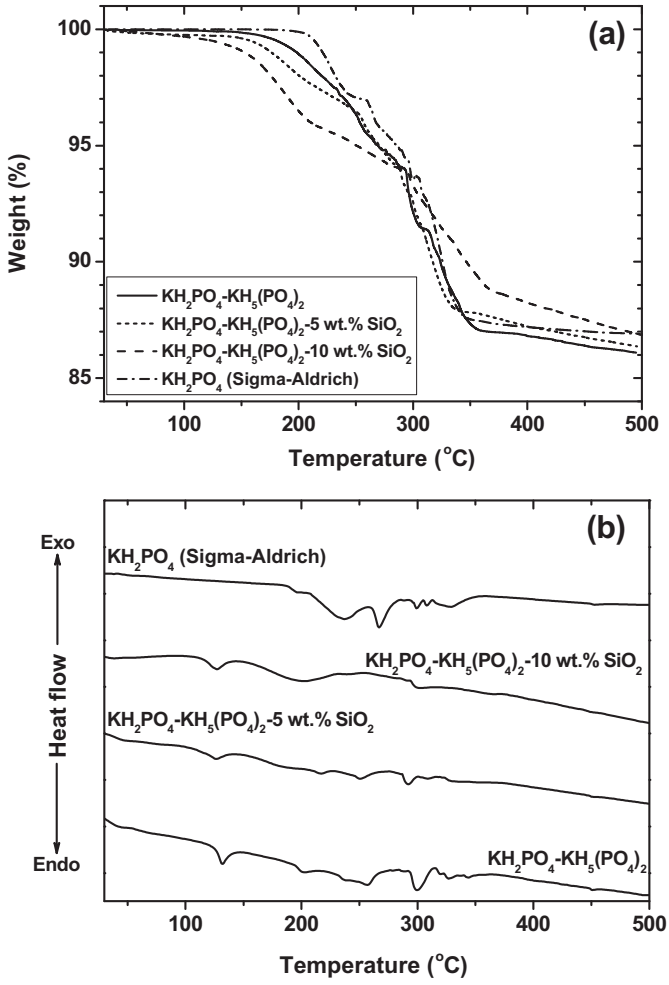

Fig. 2. (a) Thermogravimetry (TG) and (b) differential thermal analysis (DTA) of KH_2PO_4–$KH_5(PO_4)_2$–SiO_2 composites with 0 wt.%, 5 wt.%, and 10 wt.% of SiO_2 under dry Ar atmosphere.

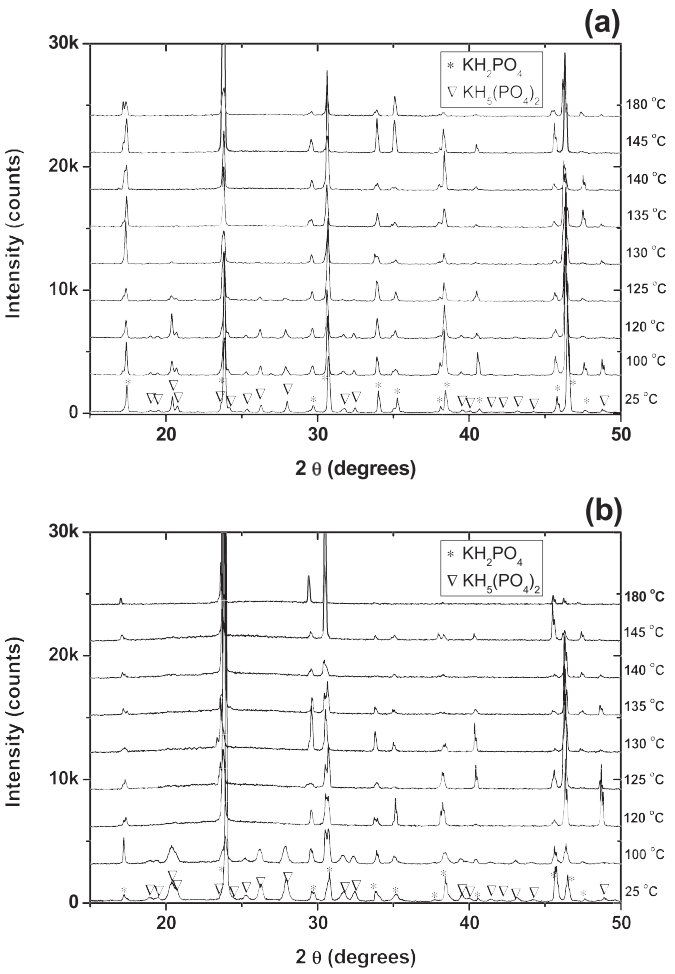

Fig. 3. High temperature X-ray diffraction patterns of (a) KH_2PO_4–$KH_5(PO_4)_2$ and (b) KH_2PO_4–$KH_5(PO_4)_2$–SiO_2 composites with 10 wt.% under dry Ar atmosphere.

The proton conductivity of KH_2PO_4–$KH_5(PO_4)_2$ under 3% H_2O/Ar is shown in an Arrhenius plot in Fig. 4 (a). The conductivity of KH_2PO_4–$KH_5(PO_4)_2$ was found to increase by about four orders of magnitude with increasing temperature from 100 °C to 140 °C, and thereafter tends to become fairly constant. Based on the trend of conductivity is in line with high-temperature X-ray diffraction and thermal analysis results, indicating that the significant increase of conductivity originates from amorphization and melting of $KH_5(PO_4)_2$. The conductivity measurement of KH_2PO_4–$KH_5(PO_4)_2$ above temperature of 140 °C is limited by the brittle nature of KH_2PO_4–$KH_5(PO_4)_2$ pellets due to partial dehydration under relatively low humidification ($pH_2O = 0.03$ atm). The conductivity data of as-received KH_2PO_4 (Sigma–Aldrich) and KH_2PO_4 in the literature [9,10] are shown in Fig. 4(a) for comparison with the as-prepared KH_2PO_4–$KH_5(PO_4)_2$, and it is found that the conductivity of pure KH_2PO_4 does not exceed 10^{-3} S·cm^{-1} in the whole measured temperature region. The results obtained in this study are consistent with a previous work [10] and indicate that the molten $KH_5(PO_4)_2$ phase plays a decisive role in increasing the proton conductivity in the directly synthesized KH_2PO_4–$KH_5(PO_4)_2$.

Fig. 4(b) shows the conductivity of KH_2PO_4–$KH_5(PO_4)_2$–SiO_2 composites with 0 wt.%, 5 wt.%, and 10 wt.% mass fractions of SiO_2 as a function of temperature. The addition of 5 wt.% and 10 wt.% SiO_2 enables conductivity measurements above a temperature of 140 °C. The temperature of the conductivity level-off is increased upon increasing the SiO_2 mass fraction, in good agreement with decrease of the onset temperature of TG and the first endothermic peak temperature of DTA curves as shown in Fig. 2. It is also notable that the conductivity of KH_2PO_4–$KH_5(PO_4)_2$–SiO_2 is similar to that of KH_2PO_4–$KH_5(PO_4)_2$ at temperature higher than 140 °C, which reflects that the molten $KH_5(PO_4)_2$ has percolated through the composite.

Fig. 5 shows the long-term conductivity of KH_2PO_4–$KH_5(PO_4)_2$–SiO_2 composites with 5 wt.% and 10 wt.% mass fractions of SiO_2 at 145 °C under a 3% H_2O/Ar atmosphere. The conductivity of the 5 wt.% SiO_2 composite undergoes a gradual decrease with time due to dehydration, while that of the 10 wt.% SiO_2 composite is stable after an initial decrease. The addition of 10 wt.% SiO_2 is found to reduce the dehydration risk of KH_2PO_4–$KH_5(PO_4)_2$, exhibiting stable conductivity for more than 70 h.

The preliminary fuel cell test using KH_2PO_4–$KH_5(PO_4)_2$–SiO_2 composite electrolyte shows an open circuit voltage of about 0.8 V for Pt/C electrodes and 0.6 V for Ag electrodes at 145 °C under H_2/Air, which is lower than the theoretical value of about 1.2 V. This observation supports that electrode reaction kinetics on the Ag electrodes is more sluggish than the Pt/C electrodes. Based on this observation, the low open circuit voltage of the cells can be attributed the poor electrode kinetics rather than the leakage of supplied gas through the electrolyte. Up to date, the state of the art electrode for solid acid fuel cell is Pt/C, hence, further study is

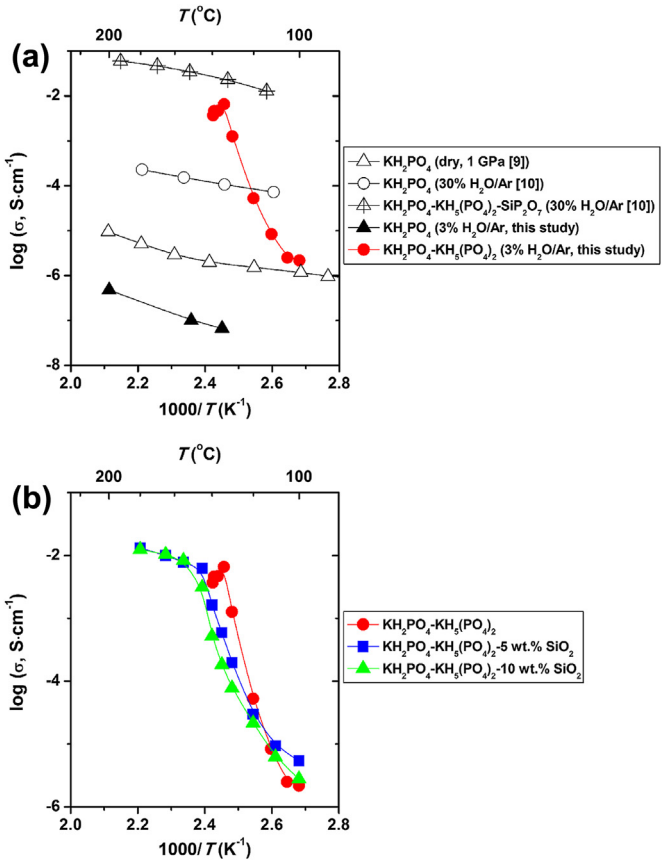

Fig. 4. (a) Temperature dependence of KH_2PO_4-based proton conductor. Also shown are data from the literature [9,10]. (b) Temperature dependence of conductivity of KH_2PO_4–$KH_5(PO_4)_2$–SiO_2 composites with 0 wt.%, 5 wt.%, and 10 wt.% of SiO_2 under 3% H_2O/Ar atmosphere.

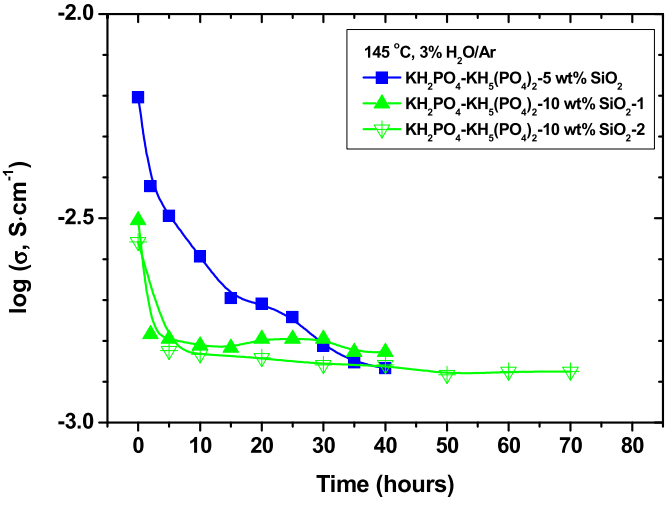

Fig. 5. Time dependence of proton conductivity of KH_2PO_4–$KH_5(PO_4)_2$–SiO_2 composites with 5 wt.% and 10 wt.% of SiO_2 under 3% H_2O/Ar atmosphere at 145 °C.

necessary to develop better electrode for solid acid based electrolyte with optimized electrode/electrolyte interface.

4. Conclusions

Proton conducting composite electrolytes based on KH_2PO_4 have been successfully prepared employing a soft chemical route, and their structural, thermal, and electrochemical properties have been systematically investigated. The findings of this study confirm that the formation of crystalline $KH_5(PO_4)_2$ in the electrolyte matrix and the melting of $KH_5(PO_4)_2$ at 130 °C enhance the conductivity of KH_2PO_4-based composite electrolytes by more than four orders of magnitude. The addition of SiO_2 is effective to improve the mechanical stability and reduce the degree of dehydration of KH_2PO_4–$KH_5(PO_4)_2$. Unlike the state of the art phosphate electrolyte (*e.g.*, CsH_2PO_4), slight humidification (pH_2O = 0.03 atm) of gas is sufficient to alleviate deterioration of the proton conductivity of KH_2PO_4–$KH_5(PO_4)_2$–SiO_2.

Acknowledgments

This work was conducted under the framework of Research and Development Program of the Korea Institute of Energy Research (KIER) (B3-2423-05). Dae Sik Yun is gratefully acknowledged for electrochemical measurements.

Appendix A. Supplementary data

Supplementary data related to this article can be found at http://dx.doi.org/10.1016/j.jpowsour.2014.03.019.

References

[1] E. Ortiz, R.A. Vargas, B.E. Mellander, Solid State Ionics 125 (1999) 177–185.
[2] J. Otomo, N. Minagawa, C. Wen, K. Eguchi, H. Takahashi, Solid State Ionics 156 (2003) 357–369.
[3] D.A. Boysen, T. Uda, C.R.I. Chisholm, S.M. Haile, Science 303 (2004) 68–70.
[4] G.V. Lavrova, E.B. Burgina, A.A. Matvienko, V.G. Ponomareva, Solid State Ionics 177 (2006) 1117–1122.
[5] A. Matsuda, T. Kikuchi, K. Katagiri, H. Muto, M. Sakai, Solid State Ionics 177 (2006) 2421–2424.
[6] Y. Taninouchi, T. Uda, Y. Awakura, Solid State Ionics 178 (2008) 1648–1653.
[7] G.V. Lavrova, V.V. Martsinkevich, V.G. Ponomareva, Inorg. Mater. 45 (2009) 795–801.
[8] A. Ikeda, D.A. Kitchaev, S.M. Haile, J. Mater. Chem. A 2 (2014) 204–214.
[9] D.A. Boysen, S.M. Haile, H. Liu, R.A. Secco, Chem. Mater. 16 (2004) 693–697.
[10] H. Muroyama, K. Kudo, T. Matsui, R. Kikuchi, K. Eguchi, Solid State Ionics 178 (2007) 1512.
[11] JCPDS File Card No. 35-0807, ICDD, PCPDFWIN v.2.4, JCPDS – International Centre for Diffraction Data, 2003.
[12] JCPDS File Card No. 23-1337, ICDD, PCPDFWIN v.2.4, JCPDS – International Centre for Diffraction Data, 2003.
[13] A. Bondarenko, W. Zhou, H.J.M. Bouwmeester, J. Power Sources 179 (2008) 380–384.
[14] V.G. Ponomareva, G.V. Lavrova, Solid State Ionics 145 (2001) 197–204.
[15] H. Shigeoka, J. Otomo, C.-J. Wen, M. Ogura, H. Takahahi, J. Electrochem. Soc. 151 (2004) J76–J83.
[16] S. Wang, J. Otomo, M. Ogura, C.-J. Wen, H. Nagamoto, H. Takahahi, Solid State Ionics 176 (2005) 755–760.
[17] V.G. Ponomareva, E.S. Shutova, Solid State Ionics 178 (2007) 729–734.
[18] G.V. Lavrova, V.G. Ponomareva, Solid State Ionics 179 (2008) 1170–1173.
[19] J. Anand Subramony, S. Lovell, B. Kahr, Chem. Mater. 10 (1998) 2053–2057.
[20] J. Anand Subramony, B.J. Marquardt, J.W. Macklin, B. Kahr, Chem. Mater. 11 (1999) 1312–1316.